



1 **Enhanced emission of intermediate/semi-volatile organic matters in both gas and**
2 **particle phases from ship exhausts with low-sulfur fuels**

3 Binyu Xiao¹, Fan Zhang^{1,2,*}, Zeyu Liu³, Yan Zhang^{4,5}, Rui Li^{1,2}, Can Wu^{1,2}, Xinyi
4 Wan¹, Yi Wang¹, Yubao Chen¹, Yong Han⁶, Min Cui⁷, Libo Zhang⁸, Yingjun Chen^{4,5},
5 Gehui Wang^{1,2,*}

6 ¹ Key Lab of Geographic Information Science of the Ministry of Education, School of
7 Geographic Sciences, East China Normal University, Shanghai, 200241, China

8 ² Institute of Eco-Chongming, 20 Cuinia Road, Chongming, Shanghai, 202150,
9 China

10 ³ State Key Laboratory of Loess and Quaternary Geology, Institute of Earth
11 Environment, Chinese Academy of Sciences, Xi'an 710061, China

12 ⁴ Shanghai Key Laboratory of Atmospheric Particle Pollution and Prevention (LAP3),
13 Department of Environmental Science and Engineering, Fudan University, Shanghai,
14 200438, China

15 ⁵ Shanghai Institute of Pollution Control and Ecological Security, Shanghai, 200092,
16 China

17 ⁶ Department of Civil and Environmental Engineering and State Key Laboratory of
18 Marine Pollution, The Hong Kong Polytechnic University, Kowloon, Hong Kong

19 ⁷ College of Environmental Science and Engineering, Yangzhou University,
20 Yangzhou, 225009, China

21 ⁸ No.1 Drilling Company, Great Wall Drilling Company, China National Petroleum
22 Corporation, Panjin, 124010, China

23 **Corresponding Authors:** Fan Zhang (fzhang@geo.ecnu.edu.cn) and Gehui Wang
24 (ghwang@geo.ecnu.edu.cn)

25 **Abstract**

26 The widespread utilization of low-sulfur fuels in compliance with global sulfur
27 limit regulations has significantly mitigated the emissions of sulfur dioxide (SO₂) and
28 particulate matter (PM) on ships. However, significant uncertainties still persist
29 regarding the impact on intermediate/semi-volatile organic compounds (I/SVOCs).
30 Therefore, on-board test of I/SVOCs from three ocean-going vessels (OGVs) and four



31 inland cargo ships (ICSs) with low-sulfur fuels ($< 0.50\%$ m/m) in China were carried
32 out in this study. Results showed that the emission factors of total I/SVOCs were $881 \pm$
33 487 , 1181 ± 421 and 1834 ± 667 mg (kg fuel)⁻¹ for OGVs with heavy fuel oil (HFO),
34 marine gas oil (MGO) and ICSs with 0# diesel, respectively. The transition from low-
35 sulfur content ($< 0.50\%$ m/m) to ultra-low-sulfur content ($< 0.10\%$ m/m) fuels had
36 evidently enhanced the emission factor of I/SVOCs, with non-ignorable contribution
37 from particle-phase I/SVOCs, thereby further amplifying the secondary organic aerosol
38 formation potential (SOAFP). Fuel type, engine type, and operating conditions
39 comprehensively influenced the emission factor level, composition, and volatility
40 distribution of I/SVOCs. Notably, a substantial proportion of fatty acids had been
41 identified in ship exhausts, necessitating heightened attention. Furthermore, organic
42 diagnostic markers of hopanes, in conjunction with the C_{18:0} to C_{14:0} acid ratio, could
43 be considered as potential markers for HFO exhausts. The findings suggest that there is
44 a necessity to optimize the implementation of a global policy on ultra-low-sulfur oil in
45 the near future.

46 **Keywords:** ship emission, I/SVOCs, low-sulfur fuel, SOAFP

47 **1 Introduction**

48 Ship transportation plays a critical role in global trade, as it accounts for over 80%
49 of the total cargo transport worldwide due to its substantial carrying capacity and cost-
50 effectiveness (Zhang et al., 2016; Zhang et al., 2021). Consequently, the expansion of
51 the global economy has led to an increasing impact on air quality, human health, and
52 various other aspects due to the emission of gaseous and particulate pollutants from
53 ship exhausts (Zhang et al., 2018a; Zhang et al., 2014; Liu et al., 2022). Over the past
54 two decades, extensive studies have been carried out on the characteristics of various
55 vessel pollutants, including sulfur dioxide (SO₂), nitrogen oxide (NO_x), particulate
56 matter (PM), carbon dioxide (CO₂) and volatile organic compounds (VOCs) (Davis et
57 al., 2001; Liu et al., 2022). Results show that shipping emissions are responsible for 2-
58 5% of fine particulate matter (PM_{2.5}) (Kramel et al., 2021); CO₂ from ships accounts
59 for around 3% of the total global CO₂ emission (Faber et al., 2020); while the NO_x from
60 ships contributes approximately 15% of the total global atmospheric NO_x emission



61 (Faber et al., 2020). Besides, the employment of high-sulfur fuel (HSF, $\geq 0.50\%$ m/m)
62 has resulted in a significant emission of SO₂ from ship exhausts, which accounts for
63 approximately 14% of global anthropogenic SO₂ emissions (Zhou et al., 2019). The
64 combustion of heavy fuel oil in ships is estimated to contribute to approximately 70%
65 of the global emissions of SO₂, leading to significant impacts on coastal areas and the
66 marine environment (International Maritime Organization, 2016).

67 Given all this, the International Maritime Organization (IMO) has been
68 continuously revising the International Convention for the Prevention of Pollution from
69 Ships (MARPOL) since 1997, progressively imposing stricter sulfur limits on marine
70 fuels. Following the guidelines of Annex VI to the MARPOL, the limit for sulfur
71 content in ship fuels has been set at 0.50% (m/m) since 2020 globally, or alternative
72 measures such as exhaust scrubbers must be employed (International Maritime
73 Organization, 2016). In designated Sulfur Emission Control Areas (SECAs, including
74 the North Sea, the Baltic Sea, North America and the United States Caribbean), this
75 limit has been further restricted to below 0.10% (m/m) since 2015. In certain SECAs,
76 the utilization of exhaust scrubbers as an alternative treatment method to low-sulfur fuel
77 is not even acceptable. Numerous countries are undergoing a transition in their shipping
78 practices, shifting from high-sulfur fuels to low-sulfur or ultra-low sulfur alternatives
79 (Liu et al., 2019; Zhang et al., 2024; Zhang et al., 2021). Within China, emission
80 standards vary across regions, with specific requirements tailored to each area.
81 Typically, the fuel oil regulations of China may mandate vessels to maintain sulfur
82 content at below either 0.50% (m/m) in SECAs since 2019 or 0.10% (m/m) in inland
83 areas and specific control regions since 2020 when utilizing fuel. In brief, the global
84 mandatory use of ultra-low sulfur content fuel ($< 0.1\%$ m/m) or alternative measures is
85 an inevitable trend in the near future.

86 Previous studies have indicated that the low-sulfur fuel regulation is an effective
87 measure for reducing SO₂ and PM emission in many countries. For example, Lehtoranta
88 et al. (2019) demonstrate that the change of fuel from high-sulfur to lower-sulfur has
89 significantly decreased the PM emissions. The global shipping emissions have been
90 quantified by Sofiev et al. (2018) using the Ship Traffic Emissions Assessment Model



91 (STEAM). Their finding reveals a positive correlation between the implementation of
92 sulfur reduced fuel strategy and reductions in both SO₂ and PM levels. However, even
93 though studies have shown that the low-sulfur fuel policy may reduce emissions of PM
94 and SO₂, it could lead to increase of VOCs and intermediate volatile organic compounds
95 (IVOCs) (Sofiev et al., 2018;He et al., 2022a;Shen et al., 2023;Liu et al., 2022). The
96 impact of fuel quality on organic compounds, such as VOCs and intermediate/semi-
97 volatile organic compounds (I/SVOCs), remains significant uncertainty.

98 VOCs have been getting lots of interests due to their crucial role as common
99 precursors of secondary organic aerosols (SOAs) and ozone (O₃) (Shen et al., 2023;Hui
100 et al., 2019). Recently, numerous studies have unveiled a substantial gap between
101 measured SOAs and theoretical calculated SOAs, with the primary cause being
102 attributed to the neglect of I/SVOCs (Fang et al., 2021;Knote et al., 2015). For example,
103 the study conducted by An et al. (2023) integrates an emission inventory of I/SVOCs
104 into the Community Multiscale Air Quality (CMAQ) modeling system to simulate the
105 characteristics of primary organic aerosols (POA) and SOAs originating from various
106 sources within the Yangtze River Delta (YRD) region. Their findings reveal a
107 significant 148% increase in predicted SOA concentrations. Wu et al. (2019) employ
108 WRF-Chem to organize the 2010 I/SVOCs emission inventory in Pearl River Delta
109 (PRD) region of China, revealing a substantial 161% increase in SOA concentration.
110 However, there is still a significant dearth of measured I/SVOCs from various sources,
111 leading to substantial uncertainty in the estimation of inventory and estimation of SOAs.

112 In recent years, several studies have reported measured data of organic compounds
113 with varying volatility emitted from ships. Although progress has been achieved in
114 shipping I/SVOCs measurement, a comprehensive understanding of their
115 characteristics and their contribution to SOA formation remains insufficient,
116 particularly in light of increasingly stringent global emission control regulations.
117 Previous studies mainly focus on gas-phase VOCs and IVOCs, which might
118 underestimate the emissions of particle-phase I/SVOCs (Huang et al., 2018a;Zhang et
119 al., 2018b;Zhang et al., 2024). Particulate I/SVOCs can also form SOA after being
120 transferred to the gaseous state through evaporation and undergoing atmospheric



121 oxidation (Srivastava et al., 2022;Liu et al., 2022). And the qualitative analysis of
122 particle-phase I/SVOCs in ship exhaust focuses more on detecting and evaluating of n-
123 alkanes and 16 polycyclic aromatic hydrocarbons (PAHs) based on limited previous
124 studies, with little emphasis on other species of I/SVOCs (Liang et al., 2022;Perrone et
125 al., 2014). There is a lack of simultaneous measurement data on detailed low-volatility
126 organic compounds in both gas and particle phases, which could be beneficial to the
127 accurate evaluation of SOA and O₃ formation potentials. Moreover, the effects resulting
128 from the implementation of low-sulfur fuel policies on shipping I/SVOC emission
129 characteristics remain unclear, particularly regarding the utilization of ultra-low sulfur
130 fuels ($\leq 0.1\%$, m/m). There is an urgent need to update emission factors and component
131 profiles of full-volatility particulate organic compounds, as this is crucial for reducing
132 uncertainties in I/SVOCs inventory estimation and providing fundamental data for
133 formulating optimal emission control policies for ships, considering their
134 comprehensive impacts on various pollutants.

135 Therefore, typical ocean-going vessels (OGVs) and inland cargo ships (ICSs) with
136 different types of fuels in China were selected for on-board measurement in this study.
137 Gas-phase and particle-phase I/SVOCs were collected synchronously from ship
138 exhausts with different low-sulfur fuels under different engine conditions. A
139 comprehensive analysis was conducted on the emission factor, volatility, profile, and
140 influence factors of I/SVOCs. Besides, the SOA formation potential (SOAFP) of
141 I/SVOCs from the test ships were also estimated based on the measured data.

142 **2 Material and methods**

143 **2.1 Test Ships and Fuels**

144 On-board test of seven typical Chinese cargo ships have been carried out in this
145 study, including three large ocean-going vessels and four small inland cargo ships.
146 Detailed comprehensive parameters of the test ships can be found in Table S1. The
147 OGVs were equipped with two types of engines, one was two-stroke main engine (ME)
148 and the other was four-stroke auxiliary engine (AE). Meanwhile, the ICSs only had one
149 four-stroke main engine. Low-sulfur content heavy fuel oil (HFO) and ultra-low-sulfur
150 marine gas oil (MGO) were used as fuels of OGVs, while 0# diesel with ultra-low-



151 sulfur content was used for ICS engines. The detailed parameters of fuels used in this
152 study are shown in Table S2. It should be acknowledged that all those fuels complied
153 with the latest regulations issued by both IMO and China. The engines tested in this
154 study were not equipped with any aftertreatment devices.

155 **2.2 Sampling system**

156 Real-world measurement of pollutants from vessels under different operating
157 conditions were conducted by a combined sampling system in this study. Vessel exhaust
158 in sampling was passed through a dilution system followed by various connected
159 samplers (Figure S1). Detailed information was described in previous studies (Zhang
160 et al., 2016; Zhang et al., 2024). Briefly, two separate sampling pipes were utilized to
161 direct emissions from the main engine and auxiliary engine stacks, respectively. A flue
162 gas analyzer probe (Testo 350, testo, Germany) was then inserted into the sampling pipe
163 to directly measure gaseous pollutants for online data collection (CO₂, O₂, CO, NO,
164 NO₂, SO₂). Another probe was used to extract flue gas for dilution. PM samples were
165 collected using particulate samplers, while gas samples were obtained by employing
166 polyurethane foam. In this study, the dilution ratios varied from 1 to 10 according to
167 operating conditions. A total of 64 sets of gas-phase and particle-phase I/SVOCs
168 samples were collected in this study, involving various engine types, fuels, and
169 operating modes. Offline samples were wrapped in prebaked aluminum foil and stored
170 at -20°C until analysis. Additionally, all samples were analyzed within two weeks of
171 sampling.

172 **2.3 Chemical analysis**

173 Organic matters in both gas-phase and particle-phase samples in this study were
174 analyzed by a gas chromatography - mass spectrometry (GC-MS, Agilent GC
175 7890B/MS 5977B, HP-5MS). Prior to analysis, the organic fraction was subjected to
176 the analytical method of N, O-bis (trimethylsilyl) trifluoroacetamide (BSTFA)
177 derivatization and spiked with internal standard (tridecane, 3.024 ng/uL). The
178 qualitative analysis was conducted using the National Institute of Standards and
179 Technology (NIST) standard organic mass spectral library queries, in conjunction with



180 their standard compound retention time. Detailed information of analysis and detection
181 process has been described elsewhere (Li et al., 2020;Li et al., 2016).

182 A total of 76 specific I/SVOC species were identified and quantified in this study,
183 including 24 n-alkanes (C₁₂-C₃₆), 16 polycyclic aromatic hydrocarbons (PAHs), 8
184 oxygenated polycyclic aromatic hydrocarbons (OPAHs), 17 acids (13 fatty acids and 3
185 benzoic acids) and 11 hopanes. Detailed information about the identified I/SVOC
186 species were presented in Table S3. Furthermore, the quantification of branched alkanes
187 (b-alkanes) and unresolved complex mixtures (UCMs) were conducted using a
188 procedure described by previous studies (Zhao et al., 2016;Zhao et al., 2014). Given
189 the good linear relationship between carbon number and volatility of n-alkanes, relative
190 response factor (RRF) of n-alkanes were used as the surrogate for b-alkanes and UCMs
191 to estimate their concentrations. The volatility classification of each substance is
192 distinguished based on its carbon number. Generally, compounds with carbon numbers
193 of 12–22 (C₁₂-C₂₂) are classified as IVOCs, while those with carbon numbers of 23–36
194 (C₂₃-C₃₆) are considered SVOCs (Zhao et al., 2014;Fujitani et al., 2020).

195 **2.4 Emission Factor**

196 Fuel-based emission factors were provided and discussed in this study using the
197 carbon balance method. It is assumed that, under ideal conditions, all carbon in the fuel
198 will undergo complete conversion into carbon present in CO₂, CO, organic carbon (OC),
199 and elemental carbon (EC) following combustion. OC and EC were analyzed using an
200 OC/EC analyzer (Model 4, Sunshine Lab). The CO₂ emission factor was derived using
201 the following formula.:

$$202 \quad EF_{CO_2} = \frac{c_F \times \Delta(CO_2)}{\Delta(c_{CO_2}) + \Delta(c_{CO}) + \Delta(c_{OC}) + \Delta(c_{EC})} \quad (1)$$

203 where EF_{CO_2} is the emission factor of CO₂ (g (kg fuel)⁻¹); $\Delta(CO_2)$ indicates the
204 CO₂ mass level after adjustment for environmental background (g m⁻³); and c_F is the
205 carbon content of fuel (g (kg fuel)⁻¹); $\Delta(c_{CO_2})$, $\Delta(c_{CO})$, $\Delta(c_{OC})$ and $\Delta(c_{EC})$ represent
206 the mass carbon concentrations of CO₂, CO, OC and EC following the deduction of the
207 background (g m⁻³), respectively.

$$208 \quad EF_x = \frac{\Delta X_x}{\Delta CO_2} \times \frac{M_x}{M_{CO_2}} \times EF_{CO_2} \quad (2)$$



209 where EF_x (g (kg fuel)^{-1}) represents the emission factor for species
210 x ; ΔX_x and ΔCO_2 (mol m^{-3}) are the concentrations of species x and CO_2 after
211 background correcting; and M_x and M_{CO_2} express the molecular weights of species x
212 and CO_2 , respectively.

213 **2.5 SOA formation potential**

214 The organic compounds in this study were categorized into two classes based on
215 volatility: Bin12-22 were defined as IVOCs, and Bin23-36 were defined as SVOCs,
216 corresponding to C12-22 and C23-36, respectively. The equation utilized for the
217 estimation of SOA production via IVOCs in this study is as follows:

$$218 \quad \Delta SOA_{IVOCs} = \sum_j [HC_j] \left(1 - e^{-k_{OH,j}^{[OH]}\Delta t}\right) \times Y_j \quad (3)$$

219 where $[HC_j]$ represents the concentration of IVOCs species involved in the
220 reaction, Y_j is the yield coefficient of IVOCs species, and k_{OH} is the reaction constant
221 of OH radicals, the specific values of Y_j and k_{OH} under different environmental
222 conditions were obtained from the simulation study of smoke chamber (Table S4-S5).

223 The equation for estimating SOA yield based on SVOCs is as follows:

$$224 \quad \Delta SOA_{SVOCs} = \sum_j (\Delta X_j \cdot Y_j) \quad (4)$$

225 where ΔX_j is the reaction mass of the compound in the j interval after partitioning,
226 based on its saturation concentration, and Y_j is the respective SOA yield. The study
227 employed a conservative calculation method and identified the UCM as the n-alkane
228 component with the lowest SOA yield. Additionally, the yield coefficients of C23 and
229 higher, which were not included in the relevant parameters, were cautiously replaced
230 with those of C22.

231 **2.6 Quality Assurance and Quality Control**

232 PAHs stipulated by EPA in the United States were used for recovery experiments,
233 and the recovery rate of PAHs was 82% ~ 115%. Before conducting GC-MS
234 measurements, n-hexane was injected prior to each measurement in order to ensure a
235 stable baseline and clean column. Subsequently, standard samples were introduced into
236 the instrument for calibration purposes. The quantitative error of the target compound
237 concentration was ensured to be less than 5% by randomly re-testing one sample after



238 every 20 samples. Moreover, the calibration of target compounds was performed
239 through simultaneous measurement of blank samples to eliminate any potential
240 experimental contamination.

241 **3 Results and discussion**

242 **3.1 Emission factors for total I/SVOCs ($EF_{I/SVOCs}$)**

243 Figure 1 presents the total $EF_{I/SVOCs}$ in both gas and particle phases for OGVs and
244 ICSs under different engine types and fuels. Obviously, OGVs had lower I/SVOCs
245 emission factors than ICSs. The average total EF_{IVOCs} of OGVs and ICSs were $512 \pm$
246 $292 \text{ mg (kg fuel)}^{-1}$ and $784 \pm 517 \text{ mg (kg fuel)}^{-1}$, respectively. While the average total
247 EF_{SVOCs} of OGVs and ICSs were $520 \pm 268 \text{ mg (kg fuel)}^{-1}$ and $1050 \pm 817 \text{ mg (kg fuel)}^{-1}$,
248 respectively. The ICSs with 0# diesel exhibited the highest level of IVOC emissions
249 ($784 \pm 587 \text{ mg (kg fuel)}^{-1}$), followed by OGVs with MGO ($651 \pm 367 \text{ mg (kg fuel)}^{-1}$),
250 while OGVs with HFO showed the lowest levels ($373 \pm 218 \text{ mg (kg fuel)}^{-1}$). When it
251 came to SVOCs, ICSs with 0# diesel ($1050 \pm 817 \text{ mg (kg fuel)}^{-1}$) was still the highest,
252 followed by OGVs with MGO ($530 \pm 170 \text{ mg (kg fuel)}^{-1}$), and OGVs with HFO ($509 \pm$
253 $365 \text{ mg (kg fuel)}^{-1}$) still showed the lowest level. It could be seen that the switch of fuels
254 from HFO to MGO had enhanced both the emission of IVOCs and SVOCs.

255 Recently, IVOCs from ships have gained more and more attentions. The average
256 EF_{IVOCs} in this study exhibited a comparable yet slightly diminished level when
257 compared to previous on-board measurement results obtained from OGVs. For instance,
258 Huang et al. (2018a) quantified the IVOCs from an OGV and showed that the total
259 EF_{IVOCs} was $1003 \text{ mg (kg fuel)}^{-1}$. The average EF_{IVOCs} from low-sulfur fuel was 2.4
260 times higher than that from high-sulfur fuel. The IVOCs data measured from the same
261 tested OGVs in this study were also provided by Liu et al. (2022), revealing EF_{IVOCs} of
262 1830.5 and $1494.4 \text{ mg (kg fuel)}^{-1}$ for MGO and HFO, respectively. It is noting that the
263 EF_{IVOCs} measured in this study was lower compared with results from Liu et al. (2022),
264 which was mainly due to different analysis methods. The thermo desorption - gas
265 chromatography /mass spectrometry (TD-GC/MS) method was employed for the
266 analysis of IVOCs extracted from adsorption tubes in the study conducted by Liu et al.
267 (2022). While in order to maximize the identification of species, this study employed

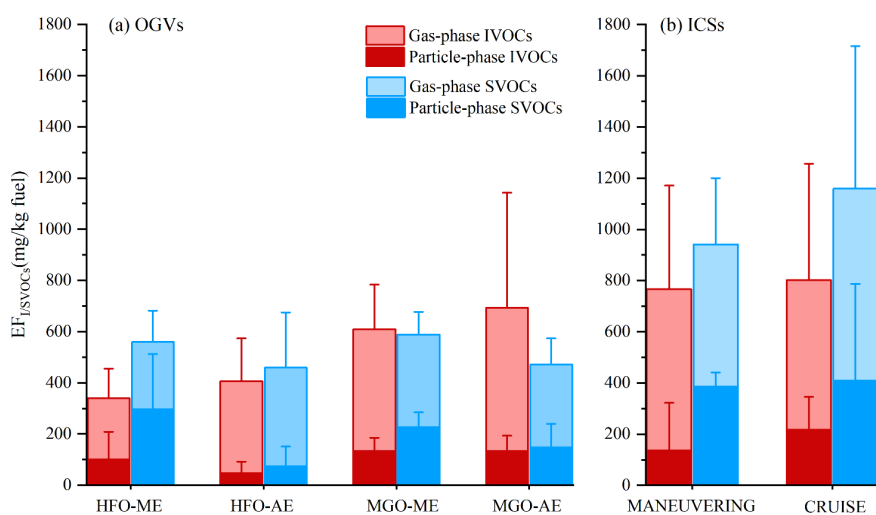


268 organic solvent extraction coupled with BSTFA derivatization method; however, it is
269 important to note that this approach may potentially underestimate the total IVOCs.
270 Other studies also reported EF_{IVOCs} from different ship engines with different fuels. For
271 instance, Lou et al. (2019) conducted a study on the gaseous IVOCs emitted from a
272 main ship engine using HFO, and demonstrated that the EF_{IVOCs} ranged from 20.2 to
273 201 mg (kg fuel)⁻¹ on average. Su et al. (2020) conducted a series of tests on fuels of
274 waste cooking oil (WCO) and MGO at the auxiliary engine test bench. They found that
275 the total EF_{IVOCs} of MGO and WCO were 2.33 ± 0.43 mg (kg fuel)⁻¹ and 1.47 ± 0.17
276 mg (kg fuel)⁻¹, respectively at the 75% of engine load. The findings from these studies
277 have demonstrated that the emission of IVOCs from ships can be influenced by a
278 multitude of influence factors, encompassing vessel types, fuel compositions, and
279 navigation conditions. However, limited research has been conducted on the
280 comprehensive emission factor of SVOCs and their constituents emitted from ships,
281 which also needs to gain more attention due to their non-negligible contribution to SOA
282 and O₃ formation (Robinson et al., 2007).

283 Figure 1 also illustrates the gas-particle partitioning of I/SVOCs from ship
284 exhausts in this study under low dilution ratios. Results showed that almost all I/SVOCs
285 in gas-phase had higher emission levels compared to particle-phase except for SVOCs
286 in HFO-ME. Previous studies focused on gaseous I/SVOC emissions of ship exhausts
287 and indicated that the gas-phase I/SVOCs played a crucial role in atmospheric chemical
288 reactions and aerosol formation processes (Liu et al., 2022; Lou et al., 2019). However,
289 the contribution of I/SVOCs from particles still could not be ignored. For example, the
290 contribution of particle-phase I/SVOCs to the total I/SVOCs could reach 16%-50% in
291 this study. Previous study has shown that they could continue to contribute to the
292 formation of SOA and O₃ largely through evaporation and oxidation in the atmosphere
293 (Drozd et al., 2021). Even though particle-phase reactions generally occur slower than
294 gas-phase reactions due to limitations imposed by oxidant diffusion and absorption into
295 aerosols (An et al., 2023), it still could be implied that particle-phase I/SVOCs were
296 similarly important precursors of SOA and O₃. The emissions of total I/SVOCs from
297 ships in both gas and particle phases should be thoroughly considered, as this could



298 potentially enhance the accuracy of simulation results for the formation of SOA and O₃.



299

300 Figure 1 Emission factors of I/SVOCs in both gas-phase and particle-phase for

301

OGVs and ICSs

302

3.2 Influence factors of I/SVOCs

303

304

305

306

307

308

309

310

311

312

313

314

315

316

317

The EFs for I/SVOCs emitted from ship exhausts exhibited significant variations under real-world conditions, as illustrated in Figure 1. In order to explore the impact of low sulfur fuel policy on I/SVOCs, EF_{I/SVOCs} with different oil products (HFO, MGO, and 0# diesel) were given and discussed in this study (seen in Figure 2 (a)). Besides, EF_{I/SVOCs} across diverse engine types (main engine (ME) and auxiliary engine (AE)), as well as various operating conditions (25%-90% operating modes of OGVs, cruise and maneuvering of ICSs) were also investigated (seen in Figure 2 (b) and (c)). Results showed that fuel type had considerable impact on the emission of I/SVOCs (Figure 2 (a)). EF_{I/SVOCs} with 0# diesel presented the highest levels, followed by MGO, while HFO had the lowest EF_{I/SVOCs}. The mean EF_{I/SVOCs} of 0# diesel, MGO, and HFO were 1834 ± 667 , 1181 ± 421 and 881 ± 487 mg (kg fuel)⁻¹, respectively. The observation was noteworthy that a decrease in sulfur content of the fuel corresponded to an increase in EF_{I/SVOCs} levels, as demonstrated by this study. Furthermore, relevant studies have also shown that the transition from high-sulfur to low-sulfur fuels resulted in an elevation of emission factors for both VOCs and IVOCs. For instance, Wu et al. (2020)



318 reported a 15-fold increase in EF_{VOCs} following the transition from high-sulfur ($>0.5\%$
319 m/m) to low-sulfur fuels, subsequent to the implementation of the low-sulfur policy.
320 Zhang et al. (2021), Huang et al. (2018a) and Liu et al. (2022) also found negative
321 correlations between sulfur content in fuel and IVOC emissions from ships. Study by
322 An et al. (2023) in the Yangtze River Delta region found that both I/SVOCs and non-
323 methane hydrocarbons (NMHCs) with low-sulfur oil had higher emission factors,
324 which resulted in a high SOA formation potential. This meant that even though the use
325 of lower sulfur content of fuels contributed to significant reduction in SO_x and PM
326 emissions and mitigated their impact on environment. It also could lead to higher
327 emissions of full-volatility organics during combustion, which had negative impacts on
328 the formation of SOA and O_3 that further affected human health. The findings suggest
329 that there is a need for optimization in the future implementation of a globally uniform
330 ultra-low-sulfur oil policy.

331 Fuel composition could directly affect the emission characteristics of I/SVOCs.
332 During the combustion of fuel, the generation of I/SVOCs could involve complex
333 processes, such as pyrolysis of organic matters, dehydrogenation, oxygenation and
334 incomplete combustion (Akherati et al., 2019;Zhao et al., 2014). A large portion of
335 I/SVOCs derived directly from incomplete combustion of fuel (Zhang et al., 2016;Liu
336 et al., 2022). The main components of 0# diesel are typically hydrocarbons, including
337 alkanes, cycloalkanes, and aromatic hydrocarbons. These components are mostly
338 within the range of I/SVOCs, mainly composed of complex hydrocarbons ranging from
339 C_{12} to C_{22} (Alam et al., 2018). The similar composition of 0# diesel to I/SVOCs might
340 be the primary reason for its highest emission levels. MGO and HFO both belong to
341 marine fuel oil (Corbin et al., 2018). MGO is a kind of light marine diesel, while HFO
342 refers to the black, viscous residue left after distilling lighter fractions such as gasoline,
343 kerosene, and diesel from crude oil, or a blend of the black, viscous residue with lighter
344 fractions (Schüppel and Gräbner, 2024). HFO are categorized into HSF and low-sulfur
345 fuel (LSF). HSF were generally utilized before low-sulfur standards were introduced,
346 while LSF have been adopted since these standards were enacted, enabling compliance
347 with stricter environmental regulations through reduced sulfur content. Unless



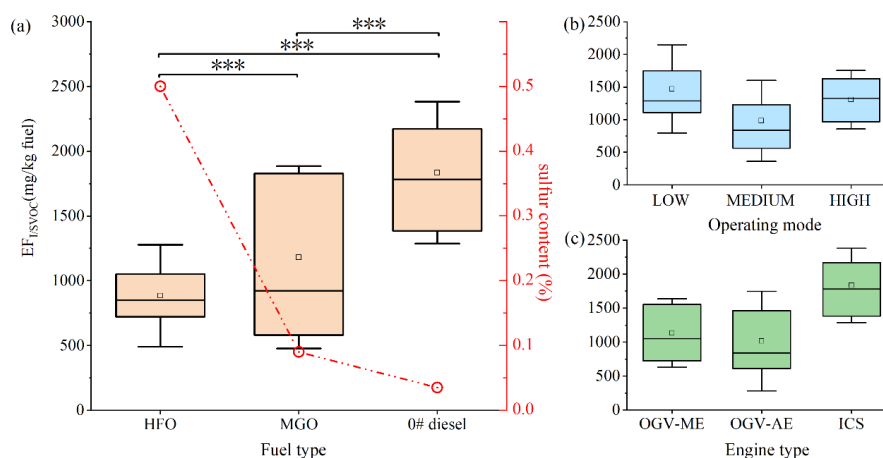
348 otherwise specified, HFO in this study refers to LSF-HFO. Referred to the measured
349 organic compositions of MGO and HFO from Liu et al. (2022), it could be seen that
350 MGO had higher n-alkanes but lower PAHs compared with HFO. This was also one
351 main reason for the higher $EF_{I/SVOCs}$ for MGO than HFO. Moreover, sulfides play a
352 catalytic role in combustion, reducing the ignition temperature of the fuel (Ju and Jeon,
353 2022). The ignition point of low-sulfur fuel is comparatively higher than that of high-
354 sulfur fuel, thereby necessitating elevated temperatures and increased oxygen input to
355 achieve complete combustion (Dinamarca et al., 2014; Drozd et al., 2019). Therefore,
356 the incomplete combustion might be enhanced for low-sulfur fuel at similar engine
357 loads (Zhao et al., 2015), leading to greater production of I/SVOCs for low-sulfur fuel.

358 The operating condition was another important factor that affected ship I/SVOCs
359 emissions. During actual navigation of OGVs, the operating modes were ranging from
360 engine load of 25% to 90%. In this study, the operating modes were categorized into
361 three distinct levels: low mode for engine loads below 50%, medium mode for loads
362 between 50% and 75%, and high mode for loads exceeding 75%. As for the ICSs,
363 because the time for departure and docking could be neglected compared with long-
364 distance cargo transportation, cruise and maneuvering were selected according to the
365 actual operating conditions. The engine operating load was higher in cruise mode
366 (classified as high mode) compared with maneuvering (medium mode). It could be seen
367 from Figure 2 (b) that the average emission factors for I/SVOCs were 1470 ± 492 mg
368 $(\text{kg fuel})^{-1}$, 982 ± 463 mg $(\text{kg fuel})^{-1}$ and 1307 ± 338 mg $(\text{kg fuel})^{-1}$ in low, medium
369 and high operating modes, respectively in this study, meaning the ships had higher
370 $EF_{I/SVOCs}$ levels at low and high operating modes, while the lowest $EF_{I/SVOCs}$ occurred
371 at medium operating modes. This was consistent with results of previous studies about
372 IVOCs from ship exhausts (Zhao et al., 2014; Huang et al., 2018b). Operating modes
373 affect the combustion state in engines, the air-fuel ratio during the combustion process,
374 thereby influencing exhaust emissions (Shrivastava and Nath Verma, 2020). Poor
375 mixing state of air and fuel at low loads leads to decreased temperature and pressure
376 during fuel combustion (Zhao et al., 2021), which in turn leads to incomplete
377 combustion of fuel. The high operating mode is associated with reduced fuel diffusion



378 and combustion time, leading to a partial oxygen deficiency within the cylinder, thereby
379 resulting in an increased generation of I/SVOCs (Zhao et al., 2016;Liu et al., 2022).
380 The investigation of methodologies for optimizing engine design and control systems
381 to achieve enhanced combustion efficiency under extreme operating conditions, thus
382 reducing emissions, is of great significance.

383 Engine type also led to difference of I/SVOC emissions from ships. There were
384 two types of engines on the OGVs, which were low-speed engines (LSE) for the main
385 engines (ME) and medium-speed engines (MSE) for the auxiliary engines (AE). While
386 only one type engine on the ICSs as the main engines, which were high-speed engines
387 (HSE) (seen in Table S1). The findings indicated that there were no statistically
388 significant differences in the $EF_{I/SVOCs}$ among various engines. Typically, medium-
389 speed engines exhibit lower combustion efficiencies than low-speed engines, leading to
390 higher I/SVOC emissions (Wu et al., 2020;Liu et al., 2022). However, because as AEs,
391 the MSEs used in this study were almost operated in medium loads that always
392 presented the lowest pollutants as described above, which resulted in the lowest
393 I/SVOC emissions as well. This finding suggested that the influence of operating
394 conditions offset that of engine type, ultimately resulting in similar levels of
395 $EF_{I/SVOCs}$ for the MSE compared to the LSE. $EF_{I/SVOCs}$ for ICSs with high-speed
396 engines presented the highest level ($1370 \pm 382 \text{ mg (kg fuel)}^{-1}$). As previously
397 mentioned, high-speed engines typically exhibit lower combustion efficiencies
398 compared to other engine types (Wu et al., 2020), while the utilization of low-sulfur
399 fuel also results in elevated levels of $EF_{I/SVOCs}$. Therefore, both the engine type and fuel
400 type used for ICSs jointly caused the highest $EF_{I/SVOCs}$ in this study.



401

402 Figure 2 Box-whisker plots of total EF_{1/SVOCs} for the tested ships under (a) different
403 fuel types, (b) different operating modes, and (c) different engine types. The error bars
404 represent the standard deviation of the measured values, while *** indicates a
405 significance level of $p < 0.001$.

406 3.3 Chemical compositions and profiles of I/SVOCs

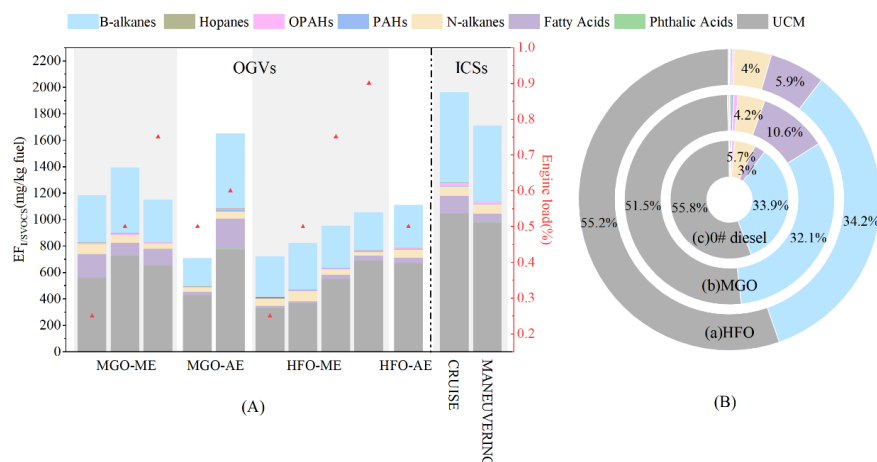
407 3.3.1 Chemical compositions of I/SVOCs

408 The chemical composition (speciated I/SVOCs and UCM) of I/SVOCs emitted
409 from OGVs and ICSs under various operating conditions are presented in Figure 3. The
410 speciated I/SVOCs included n-alkanes, branched alkanes (b-alkanes), (O)PAHs,
411 hopanes and acids. In general, UCM and b-alkanes dominated the total I/SVOCs from
412 ship exhausts, contributing 83.4% to 89.8% of the total I/SVOCs (speciated + UCMs).
413 The emissions of acids and n-alkanes were also noteworthy, accounting for average of
414 6.51% and 4.61% of the total I/SVOCs, respectively. Previous studies also have noted
415 the relatively high proportion of n-alkanes in I/SVOCs from shipping emission sources
416 (Huang et al., 2018a; He et al., 2022a). However, there is limited data available on
417 organic acids, particularly those emitted by shipping activities. PAHs, hopanes, and
418 benzoic acids collectively contribute only about 1% to the overall emissions, indicating
419 their relatively minor role. However, even though these substances only constituted a
420 small proportion of the overall emissions, the environmental and health effects still
421 demanded in-depth research and vigilance due to their strong toxicity and bio-



422 accumulative nature (He et al., 2022b;Mochida et al., 2003).

423 It is noteworthy that both the EFs and proportions of fatty acids in the total
424 I/SVOCs were found to be remarkably high in this study, as previously mentioned. This
425 finding aligns with the results reported by Huang et al. (2018a) and Wang et al. (2023),
426 where n-fatty acids were identified as a significant component of chemical
427 compositions derived from an OGV exhaust. However, there is still very little research
428 on fatty acids from shipping emissions. Fatty acids are a category of organic compounds
429 with carboxyl groups and relatively long carbon chains, playing essential physiological
430 roles within organisms. Prolonged exposure to elevated levels of fatty acid pollutants
431 has been linked to the development of respiratory, immune, and cardiovascular
432 disorders (He et al., 2022a;He et al., 2022b). Studies have indicated that fatty acids can
433 constitute a substantial portion of the organic matter in atmospheric aerosols, especially
434 in marine aerosols (Hu et al., 2023;Mochida et al., 2003;Kawamura et al., 2017). For
435 example, research in the North Pacific had shown that fatty acids could account for 10%
436 to 30% of organic carbon (Mochida et al., 2003;Mochida et al., 2002). In addition, low-
437 molecular-weight fatty acids (C_{14:0}-C_{19:0}) have been increasing in the North Pacific in
438 recent years (Hu et al., 2023). The content of fatty acids in marine aerosols was
439 relatively high, yet their specific sources were often attributed to biomass burning and
440 biological emissions in the past (Hu et al., 2023;Kawamura et al., 2010). It could be
441 inferred from the results in this study that shipping emission might be one significant
442 potential contributor to the fatty acids in marine aerosols. Besides, the EF of fatty acids
443 were found to be higher in ship exhausts fueled by MGO and 0# diesel compared to
444 HFO, which aligns with the findings of Huang et al. (2018a) indicating that the average
445 EF of n-fatty acids from LSF was 6.7 times greater than that from HSF. Consequently,
446 the forthcoming implementation of a globally uniform ultra-low-sulfur oil policy may
447 potentially lead to an elevated release of fatty acids, particularly in coastal and inland
448 regions. Given studies on acid pollutants from ship exhausts were relatively scarce or
449 they had been overlooked due to limitations in sampling and detection methods. Further
450 investigation is warranted to enhance the comprehension of the characteristics and
451 influences of acidic emissions derived from ship exhausts.



452

453 Figure 3 Chemical composition of I/SVOCs from the tested ships, (A) emission
454 factors and (B) distributions

455 As mentioned above, the total $EF_{I/SVOCs}$ of ship exhausts was significantly
456 influenced by fuel type. The average emission factors of the primary chemical
457 compositions of I/SVOCs under various fuel conditions are presented in Table 1.
458 Results demonstrated that the EFs of the majority of organic compounds in ship
459 emissions exhibited an upward trend as the sulfur content in fuels decreased.
460 Specifically, emission factors of UCM, branched alkanes and (O)PAHs for 0# diesel
461 were much higher than the other two fuels, with HFO having the lowest values. While
462 in terms of n-alkanes, the average total EFs of n-alkanes in these fuel types were
463 $72.9 \pm 28.1 \text{ mg (kg fuel)}^{-1}$ (0# diesel), $50.1 \pm 15.1 \text{ mg (kg fuel)}^{-1}$ (HFO) and $49.2 \pm 11.2 \text{ mg}$
464 $(\text{kg fuel})^{-1}$ (MGO), respectively, indicating a slight deviation from the findings of Liu et
465 al. (2022) regarding the higher $EF_{n\text{-alkanes}}$ in MGO compared to HFO. This might be
466 explained by that not only n-alkanes in IVOCs, but also SVOCs were detected in this
467 study. Compared with IVOCs referring from C_{12} to C_{22} , SVOCs ($C_{22}\text{-}C_{36}$) from HFO
468 had higher emission factor values due to the higher carbon chains than MGO (details
469 also have been shown in Section 3.4), which offset the higher $EF_{n\text{-alkanes}}$ caused by
470 IVOCs (seen in Figure 1). Besides, compared with the other two types of fuels, MGO
471 emitted higher emission factor level of acids. MGO is a blend of straight-run light
472 distillate diesel and secondary processed diesel from crude oil (Ahn et al., 2021), which



473 may contain a considerable amount of impurities, which could be a reason for its higher
474 content of acidic substances. However, hopanes from HFO presented the highest
475 emission factor level, which was one rare category of organic matters that decreased
476 with the improvement of fuel quality. The details will be discussed in Section 3.3.2.

477 Table 1 Average emission factors of main chemical compositions of I/SVOCs under
478 different fuels (mg (kg fuel)⁻¹).

Fuel Type	UCM	B-alkanes	Acids	N-alkanes	(O)PAHs	Hopanes
HFO	492±137	299±17.5	27.7±10.6	50.1±15.1	9.47±3.1	2.99±1.01
MGO	608±109	379±112	129±57.7	49.2±11.2	12.9±5.3	2.41±0.88
0# diesel	1010±134	628±55.7	99.5±33.9	72.9±28.1	21.4±3.3	1.88±0.82

479 3.3.2 Profiles of I/SVOCs

480 Detailed profiles of organic compounds from ship exhausts are of great
481 significance for source identification. The profile characteristics of the identified
482 organic compounds, including fatty acids, n-alkanes, PAHs, OPAHs, and hopanes
483 measured from the three types of ships in this study are presented in Figure 4. Results
484 showed that fatty acids with 11-18 carbon numbers (C_{11:0-18:0} and C_{18:1}) were the main
485 acids emitted from ships, especially *n*-C₁₄ and *n*-C₁₈. In addition, it showed that HFO
486 had a significantly lower proportion of Dodecanoic (C_{12:0}) and Tetradecanoic (C_{14:0})
487 compared with 0# diesel and MGO, while the proportion of Octadecanoic (C_{18:0}) in 0#
488 diesel was lower than other fuels. The C_{18:0} to C_{14:0} ratios of HFO, MGO and 0# diesel
489 were 3.7±1.0, 0.3±0.2 and 0.1±0.4, respectively. This C_{18:0} to C_{14:0} ratio decreased
490 significantly with the decrease of sulfur content of the fuel. Besides, the average
491 proportion of fatty acids containing an even number of carbons (88.05%±3.7%) in this
492 study was significantly higher than that of fatty acids with an odd number of carbons.
493 Previous studies have demonstrated a robust distribution of fatty acids with even-
494 numbered carbon chains in marine aerosols, exhibiting distinct peaks at *n*-C₁₆ and *n*-
495 C₁₈ (Hu et al., 2023; Kawamura et al., 2017; Mochida et al., 2002), thereby providing
496 further evidence that ship exhaust emissions constitute a significant source of fatty acids
497 in marine aerosols. Given the limited availability of studies on single-source acids, it is
498 imperative to gather additional evidence regarding acid pollution resulting from ship



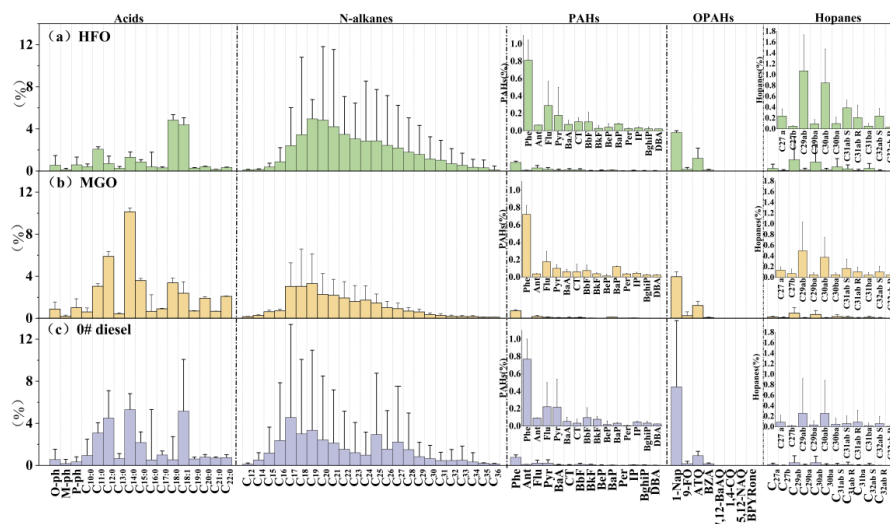
499 transportation emissions. This will enhance our comprehension of the magnitude of the
500 issue and the environmental and human health implications associated with these
501 emissions.

502 The n-alkane profiles of the three types of fuels in this study (depicted in Figure 4)
503 clearly indicated that low carbon number n-alkanes exhibit dominance. N-nonadecane
504 (C₁₉) was the highest composition for both HFO and MGO. While 0# diesel exhibited
505 a peak at heptadecane (C₁₇), which was mainly caused by the characteristic of fuel
506 composition. Significant variations were observed in the emissions of n-alkanes from
507 other non-internal combustion engine sources, such as high composition of n-
508 octacosane (C₂₉) and apparent odd-carbon advantages in biomass emissions (Hu et al.,
509 2023; Perrone et al., 2014); high composition in C₂₃ and C₂₁ for coal combustion (Duan
510 et al., 2010; Xie et al., 2009).

511 The PAH profiles associated with different fuel types in this study exhibited similar
512 patterns to those observed by Liu et al. (2022), wherein low molecular weight PAHs
513 were found to constitute a relatively higher proportion. The major compounds in this
514 study were Phenanthrene (Phe), Pyrene (Pyr), Fluorene (Flu), Chrysene (Chr) and
515 Benzo[a]pyrene (Bap), aligning with the conclusions of previous studies (Zhang et al.,
516 2016; Zhang et al., 2014). PAHs from 0# diesel had higher proportion of Pyr and lower
517 proportion of Bap compared with the other two types of fuels. Besides, high proportions
518 of 1-Naphthaldehyd (1-Nap) and Anthraquinone (ATQ) in OPAHs were also revealed
519 from ship exhausts in this study, with 1-NAP for 0# diesel having the highest level.
520 Most of the PAHs and OPAHs emitted in this study were low molecular weight tricyclic
521 and tetracyclic substances, accounting for 94.7% to 96.9% of total OPAHs + PAHs, and
522 6.6%±2.1%, 6.7%±1.7% and 10.1%±5.9% of the total speciated I/SVOC profile in
523 HFO, MGO and 0# diesel, respectively. The present study observed a positive
524 correlation between the decrease in sulfur content and an increase in OPAHs + PAHs
525 with smaller ring numbers emitted from ship exhausts, while conversely, higher ring
526 compounds exhibited a negative relationship. Specifically, 1-Nap accounted for
527 significantly higher proportion of OPAHs + PAHs in 0# diesel (70.4%±1.2%) than in
528 MGO (47.9%±7.3%) and HFO (36.6%±15.2%). As the sulfur content decreased, both



529 the emission factor level and proportion of 1-NAP exhibited an increasing trend.
 530 Hopanes are found mainly in coal, fuel oils and lubricants and are generally
 531 regarded as molecular markers of fossil fuel combustion sources due to their stable
 532 chemical property (Cass, 1998). In this study, C_{29ab} and C_{30ab} were the main hopanes
 533 emitted from ships, accounting for 67.1%±5.5% of the total hopanes. In addition, C_{31ab}
 534 s, C_{31ab} R and C_{32ab} s also showed non-ignorable contributions in ship emissions.
 535 Different from n-alkanes and (O)PAHs, among the fuels, hopanes presented the highest
 536 proportions from exhausts of HFO, followed by MGO, while 0# diesel showed the
 537 lowest levels. This finding was consistent with the results reported by Sippula et al.
 538 (2014), which demonstrated that HFO operation yields higher concentrations of
 539 hopanes compared to diesel fuel. The primary reason for this disparity was attributed to
 540 the presence of hopanes in HFO, whereas lubrication oil served as the sole source of
 541 these compounds during diesel fuel operation (Kleeman et al., 2008). Given vanadium
 542 and nickel cannot continue to be typical tracers of ship exhausts with low-sulfur content
 543 HFO (Yu et al., 2021), organic diagnostic characteristics such as hopanes coupled with
 544 the ratio of C_{18:0} to C_{14:0} could be considered as potential markers of HFO exhausts.



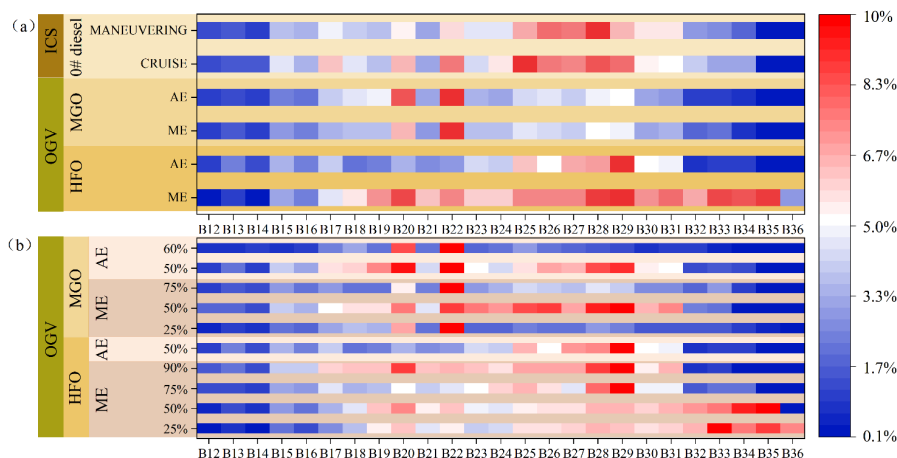
545
 546
 547

Figure 4 Profiles of I/SVOCs in ship exhausts under different fuels



548 **3.4 Volatility Distribution of I/SVOCs**

549 Volatility distribution of I/SVOCs from ships is shown in Figure 5, 24 Bins
550 were divided using n-alkanes as an indicator. What needs to illustrate was that the
551 effective saturation concentration (C^*) of n-alkanes in each bin was used as a
552 surrogate value to discuss the volatility distribution of I/SVOCs (Zhao et al.,
553 2016;Zhao et al., 2014). The employed experimental method of solvent extraction in
554 this study should be acknowledged for its potential to underestimate highly volatile
555 organic compounds. However, in the meantime, this method could also effectively
556 identify and quantify as many I/SVOC species as possible. Figure 5 shows the
557 proportion of I/SVOCs in each volatile bin to further investigate the effects of
558 different factors on I/SVOCs. Obviously, fuel type had apparent impact on the
559 overall trend of volatility distribution of $EF_{I/SVOC}$, with similar volatility profiles of
560 identical fuels (Figure 5 (a)). While operating mode and engine type also affected
561 the volatility distributions of I/SVOCs (Figure 5 (b)). For example, for both HFO-
562 ME and MGO-ME of OGVs, there were maximum values in bin 29. The range and
563 magnitude of this maximum region increased with engine load, reaching its peak at
564 50% engine load and subsequently declining at 75% engine load (Figure 5 (b)). The
565 higher emissions of I/SVOCs in low-speed and high-speed loads might be
566 significantly influenced by the increase of these low-volatile components.
567



568

569 Figure 5 Split-bar heat plot of the I/SVOCs proportions in each volatile bin under

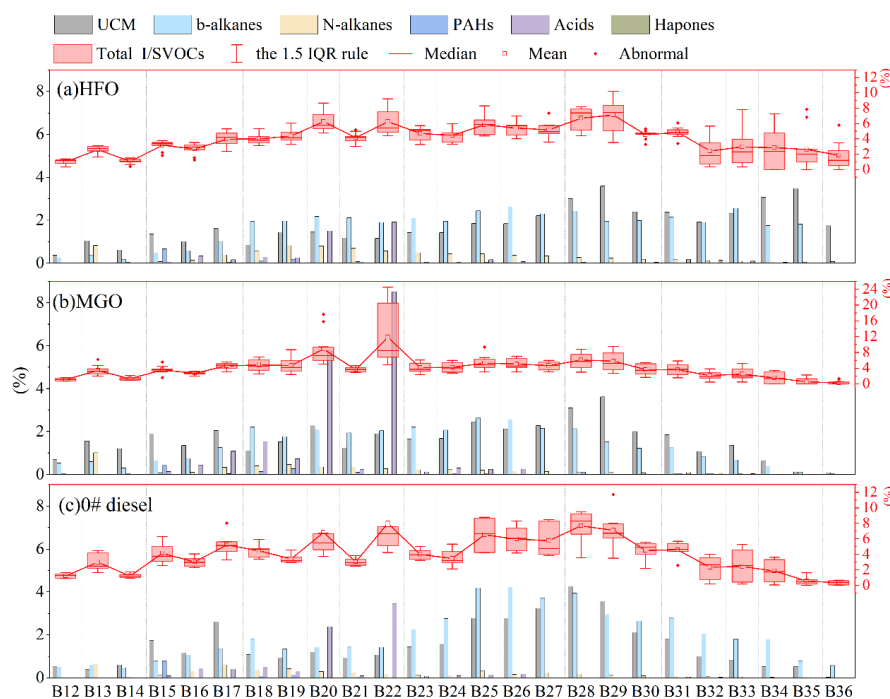
570 (a) different fuel types for different engines, and (b) different operating conditions

571 (25%-90% operating modes) for OGVs

572 In order to figure out the volatility distributions of detailed chemical compositions
573 of I/SVOCs from different fuels. The average volatility distributions of UCM, b-alkanes,
574 n-alkanes, PAHs, acids and hopanes were given in Figure 6. Results revealed that the
575 volatility distributions of UCM and b-alkanes in 0# diesel exhibited distinct bimodal
576 characteristics, with higher concentrations observed in low volatility bins
577 (approximately Bin 22-Bin 32). The peaks for UCM were in Bin 17 and Bin 29, while
578 in Bin 18 and Bin 26 for b-alkanes. However, The UCM and b-alkanes of both HFO
579 and MGO exhibited no significant peak characteristic. Compared with 0# diesel and
580 MGO, HFO also presented higher proportions of low-volatility UCMs and b-alkanes
581 after Bin 32 due to more low-volatility substances emitted. Volatile distributions of n-
582 alkanes from 0# diesel also had bimodal structure, reaching peaks at Bin 17 and Bin 27,
583 respectively. While the volatile profiles of n-alkanes from MGO and HFO showed
584 basically unimodal distributions with peaks at Bin19. Furthermore, compared with
585 HFO, more n-alkanes from MGO were emitted in high volatility regions. This was due
586 to the characteristics of the fuels that MGO and 0# diesel fractions were lower than
587 HFO fraction and had lower organic carbon numbers (Liu et al., 2022). The volatility
588 distributions of other special I/SVOCs were consistent with their molecular size.



589 (O)PAHs discharged from ships were mostly small molecules with high volatility,
590 which were enriched in Bin 15. The acids were predominantly concentrated within the
591 high volatility bins (Bin 16-Bin 22), exhibiting prominent peaks at Bin 20 and Bin 22.
592 Hopanes, on the other hand, showed a primary concentration in the low volatility
593 intervals following Bin 29. The composition and physicochemical properties of
594 different fuel types vary, leading to differences in the volatile organic compounds they
595 contain. Consequently, the type of fuel played a significant role in determining the
596 distribution of volatile fractions for each individual I/SVOC component.



597

598

599

Figure 6 The volatility distributions of I/SVOCs from different fuels

3.5 SOA formation potential of I/SVOCs

600

601

602

603

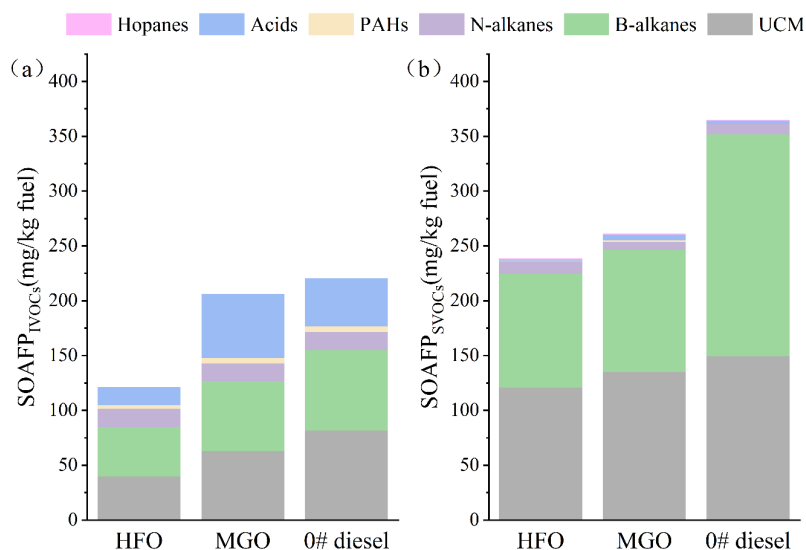
604

605

I/SVOCs have been proposed as crucial precursors of SOA (Murphy et al., 2017;Hu et al., 2023). However, most of previous studies about ship exhausts focus on the contribution of gas-phase IVOCs on SOA (Huang et al., 2018b;Liu et al., 2022), the contributions from IVOCs and SVOCs in particle-phase have been neglected. The comprehensive assessment of ship exhaust emissions, encompassing both gas-phase and particle-phase I/SVOCs, was crucial for evaluating the overall impact on the



606 environment. This became particularly important in light of the implementation of low-
607 sulfur fuel policies, which had resulted in increased emissions of full-volatility organic
608 compounds. Therefore, the SOAFPs of I/SVOCs from ships with different fuels were
609 estimated (shown in Figure 7). Results showed that in terms of the total SOAFP
610 evaluated from both IVOCs and SVOCs, 0# diesel and MGO with the lower sulfur
611 content showed higher values, which could reach as high as 634 mg (kg fuel)⁻¹ and 418
612 mg (kg fuel)⁻¹, respectively. In comparison, the SOAFP from HFO only had a lower
613 value of 354 mg (kg fuel)⁻¹. For IVOCs, the use of low-sulfur 0# diesel and MGO could
614 lead to higher SOAFP that reached 234 mg (kg fuel)⁻¹ and 157 mg (kg fuel)⁻¹
615 respectively, while HFO exhibited a significantly lower SOAFP level of only 101 mg
616 (kg fuel)⁻¹. As for SVOCs, the SOAFPs of those three fuels were 400 mg (kg fuel)⁻¹ for
617 0# diesel, 261 mg (kg fuel)⁻¹ for MGO and 253 mg (kg fuel)⁻¹ for HFO. Results from
618 this study indicated that SOAFP could be enhanced with the decrease of sulfur content,
619 the same as I/SVOCs emission factors. The major contribution to the total SOAFPs was
620 observed from B-alkanes and UCM, accounting for 81.1%-87.8%, while the
621 significance of acids, particularly IVOCs, should not be overlooked. Besides, SOAFPs
622 from SVOCs were higher than that of IVOCs, no matter what types of fuels, which
623 further indicated the importance of SVOCs. However, due the analysis method of
624 I/SVOCs, the emission factor as well as SOAFP were underestimated in this study.
625 More real-world measurement of chemically identifiable full-volatility organic matters
626 should be carried out to figure out their emission characteristics and SOAFPs,
627 especially for the ultra-low-sulfur marine fuels, which could provide basis for the
628 further establishment of ship emission policies.



629

630

631

Figure 7. SOAFP from (a) IVOCs and (b) SVOCs

4 Conclusions and atmospheric implications

632

633

634

635

636

637

638

639

640

641

642

The results revealed that $EF_{I/SVOCs}$ of ICSs were higher than OGVs. Furthermore, a decreasing sulfur content in fuel was found to be associated with an increasing trend in $EF_{I/SVOCs}$. Fuel quality, engine type, and engine load all exerted significant influences on the emissions, compositions, and volatility distributions of I/SVOCs. Besides, the most predominant I/SVOC components were UCM and b-alkanes, followed by acids and n-alkanes. Notably, a significant presence of fatty acids was detected in ship exhausts, warranting further attention, particularly towards fatty acids ranging from C_{11} - C_{18} carbon numbers. It also found that organic diagnostic markers of hopanes, in conjunction with the $C_{18:0}$ to $C_{14:0}$ acid ratio, could be considered as potential markers for HFO exhausts. Moreover, the transition from low-sulfur content to ultra-low-sulfur content fuels had also enhanced the secondary organic aerosol formation potential.

643

644

645

646

647

648

The findings of this study, along with previous research, suggest that a decrease in sulfur content in fuels leads to a significant increase in emissions of full-volatility organics from OGVs. This further exacerbates the SOAFP, which pose serious environmental and health risks, particularly in densely populated coastal areas. Therefore, there is a need for optimization of the implementation of an ultra-low-sulfur oil policy. Moreover, high proportions of acidic substances in I/SVOCs from ships were



649 found in this study, which extended the profiles of ship exhaust emissions. It also could
650 be inferred that organic diagnostic characteristics, such as hopanes, in combination with
651 the ratio of $C_{18:0}$ to $C_{14:0}$ could be considered as potential markers for HFO exhausts.
652 However, there were still limitations in this study that the experimental method used
653 might lead to the underestimation of highly volatile organic compounds. Besides, more
654 than half of the I/SVOCs still could not be identified in this study. Improved
655 experimental method needs to be considered to identify more full-volatility organic
656 substances with greater precision and accuracy in future study. Considering the proven
657 effectiveness of after-treatment systems, such as diesel oxidation catalyst (DOC), diesel
658 particulate filter (DPF), and selective catalytic reduction (SCR), in reducing emissions
659 of full-volatility organic compounds (Reşitoğlu et al., 2015;Nadanakumar et al.,
660 2021;Biswas et al., 2009;Yashnik and Ismagilov, 2023;Hamada and Haneda, 2012),
661 these systems could be regarded as potential measures to mitigate the elevated levels of
662 I/SVOCs emitted by ships.

663

664 **Author contributions:**

665 FZ, GW, YZ, and YC conceptualized and designed the study; BX, ZL, XW, YW,
666 YH, MC, and YbC performed the measurements; FZ, RL, CW, LZ, and GW analyzed
667 the data. BX wrote the manuscript draft; All the authors reviewed, edited, and
668 contributed to the scientific discussion in the manuscript.

669 **Competing interests**

670 The contact author has declared that none of the authors has any competing
671 interests.

672 **Acknowledgments**

673 This study was supported by the National Natural Science Foundation of China
674 (42377096, 42130704, U23A2030).

675 **References**

676 Ahn, S., Seo, J. M., and Lee, H.: Thermogravimetric Analysis of Marine Gas Oil
677 in Lubricating Oil, *J. Mar. Sci. Eng.*, 9, 339, 2021.
678 Akherati, A., Cappa, C. D., Kleeman, M. J., Docherty, K. S., Jimenez, J. L., Griffith,
679 S. M., Dusanter, S., Stevens, P. S., and Jathar, S. H.: Simulating secondary organic
680 aerosol in a regional air quality model using the statistical oxidation model – Part 3:



- 681 Assessing the influence of semi-volatile and intermediate-volatility organic compounds
682 and NO_x, *Atmos. Chem. Phys.*, 19, 4561-4594, 10.5194/acp-19-4561-2019, 2019.
- 683 Alam, M. S., Zeraati-Rezaei, S., Liang, Z., Stark, C., Xu, H., MacKenzie, A. R.,
684 and Harrison, R. M.: Mapping and quantifying isomer sets of hydrocarbons($\geq C_{12}$) in
685 diesel exhaust, lubricating oil and diesel fuel samples using GC \times GC-ToF-MS, *Atmos.*
686 *Meas. Tech.*, 11, 3047-3058, 10.5194/amt-11-3047-2018, 2018.
- 687 An, J., Huang, C., Huang, D., Qin, M., Liu, H., Yan, R., Qiao, L., Zhou, M., Li, Y.,
688 Zhu, S., Wang, Q., and Wang, H.: Sources of organic aerosols in eastern China: a
689 modeling study with high-resolution intermediate-volatility and semivolatile organic
690 compound emissions, *Atmos. Chem. Phys.*, 23, 323-344, 10.5194/acp-23-323-2023,
691 2023.
- 692 Biswas, S., Verma, V., Schauer, J. J., and Sioutas, C.: Chemical speciation of PM
693 emissions from heavy-duty diesel vehicles equipped with diesel particulate filter (DPF)
694 and selective catalytic reduction (SCR) retrofits, *Atmos. Environ.*, 43, 1917-1925,
695 <https://doi.org/10.1016/j.atmosenv.2008.12.040>, 2009.
- 696 Cass, G. R.: Organic molecular tracers for particulate air pollution sources, *Trac-*
697 *Trends in Analytical Chemistry*, 17, 356-366, 10.1016/s0165-9936(98)00040-5, 1998.
- 698 Corbin, J. C., Pieber, S. M., Czech, H., Zanatta, M., Jakobi, G., Massabò, D.,
699 Orasche, J., El Haddad, I., Mensah, A. A., Stengel, B., Drinovec, L., Mocnik, G.,
700 Zimmermann, R., Prévôt, A. S. H., and Gysel, M.: Brown and Black Carbon Emitted
701 by a Marine Engine Operated on Heavy Fuel Oil and Distillate Fuels: Optical Properties,
702 Size Distributions, and Emission Factors, *J. Geophys. Res.-Atmos.*, 123, 6175-6195,
703 <https://doi.org/10.1029/2017JD027818>, 2018.
- 704 Davis, D. D., Grodzinsky, G., Kasibhatla, P., Crawford, J., Chen, G., Liu, S., Bandy,
705 A., Thornton, D., Guan, H., and Sandholm, S.: Impact of ship emissions on marine
706 boundary layer NO_x and SO₂ distributions over the Pacific basin, *Geophys. Res. Lett.*,
707 28, 235-238, Doi 10.1029/2000gl012013, 2001.
- 708 Dinamarca, M. A., Rojas, A., Baeza, P., Espinoza, G., Ibacache-Quiroga, C., and
709 Ojeda, J.: Optimizing the biodesulfurization of gas oil by adding surfactants to
710 immobilized cell systems, *Fuel.*, 116, 237-241, 10.1016/j.fuel.2013.07.108, 2014.
- 711 Drozd, G. T., Zhao, Y., Saliba, G., Frodin, B., Maddox, C., Oliver Chang, M. C.,
712 Maldonado, H., Sardar, S., Weber, R. J., Robinson, A. L., and Goldstein, A. H.: Detailed
713 Speciation of Intermediate Volatility and Semivolatile Organic Compound Emissions
714 from Gasoline Vehicles: Effects of Cold-Starts and Implications for Secondary Organic
715 Aerosol Formation, *Environ. Sci. Technol.*, 53, 1706-1714, 10.1021/acs.est.8b05600,
716 2019.
- 717 Drozd, G. T., Weber, R. J., and Goldstein, A. H.: Highly Resolved Composition
718 during Diesel Evaporation with Modeled Ozone and Secondary Aerosol Formation:
719 Insights into Pollutant Formation from Evaporative Intermediate Volatility Organic
720 Compound Sources, *Environ. Sci. Technol.*, 55, 5742-5751, 10.1021/acs.est.0c08832,
721 2021.
- 722 Duan, F., He, K., and Liu, X.: Characteristics and source identification of fine
723 particulate n-alkanes in Beijing, China, *JEnvS*, 22, 998-1005, 10.1016/s1001-
724 0742(09)60210-2, 2010.
- 725 Faber, J., Hanayama, S., Zhang, S., Pereda, P., Comer, B., Hauerhof, E., van der
726 Loeff, W. S., Smith, T., Zhang, Y., and Kosaka, H.: Fourth IMO GHG Study, London,
727 UK, 2020.
- 728 Fang, Z., Li, C., He, Q., Czech, H., Groger, T., Zeng, J., Fang, H., Xiao, S., Pardo,
729 M., Hartner, E., Meidan, D., Wang, X., Zimmermann, R., Laskin, A., and Rudich, Y.:
730 Secondary organic aerosols produced from photochemical oxidation of secondarily



- 731 evaporated biomass burning organic gases: Chemical composition, toxicity, optical
732 properties, and climate effect, *Environ. Int.*, 157, 106801,
733 10.1016/j.envint.2021.106801, 2021.
- 734 Fujitani, Y., Sato, K., Tanabe, K., Takahashi, K., Hoshi, J., Wang, X., Chow, J. C.,
735 and Watson, J. G.: Volatility Distribution of Organic Compounds in Sewage
736 Incineration Emissions, *Environ. Sci. Technol.*, 54, 14235-14245,
737 10.1021/acs.est.0c04534, 2020.
- 738 Hamada, H., and Haneda, M.: A review of selective catalytic reduction of nitrogen
739 oxides with hydrogen and carbon monoxide, *Applied Catalysis A: General*, 421-422, 1-
740 13, <https://doi.org/10.1016/j.apcata.2012.02.005>, 2012.
- 741 He, X., Zheng, X., You, Y., Zhang, S. J., Zhao, B., Wang, X., Huang, G. H., Chen,
742 T., Cao, Y. H., He, L. Q., Chang, X., Wang, S. X., and Wu, Y.: Comprehensive chemical
743 characterization of gaseous I/SVOC emissions from heavy-duty diesel vehicles using
744 two-dimensional gas chromatography time-of-flight mass spectrometry, *Environ.*
745 *Pollut.*, 305, ARTN 119284
746 10.1016/j.envpol.2022.119284, 2022a.
- 747 He, X., Zheng, X., Zhang, S., Wang, X., Chen, T., Zhang, X., Huang, G., Cao, Y.,
748 He, L., Cao, X., Cheng, Y., Wang, S., and Wu, Y.: Comprehensive characterization of
749 particulate intermediate-volatility and semi-volatile organic compounds (I/SVOCs)
750 from heavy-duty diesel vehicles using two-dimensional gas chromatography time-of-
751 flight mass spectrometry, *Atmos. Chem. Phys.*, 22, 13935-13947, 10.5194/acp-22-
752 13935-2022, 2022b.
- 753 Hu, C., Yue, F., Zhan, H., Leung, K. M. Y., Zhang, R., Gu, W., Liu, H., Chen, A.,
754 Cao, Y., Wang, X., and Xie, Z.: Homologous series of n-alkanes and fatty acids in the
755 summer atmosphere from the Bering Sea to the western North Pacific, *Atmos. Res.*,
756 285, 106633, <https://doi.org/10.1016/j.atmosres.2023.106633>, 2023.
- 757 Huang, C., Hu, Q., Wang, H., Qiao, L., Jing, S. a., Wang, H., Zhou, M., Zhu, S.,
758 Ma, Y., Lou, S., Li, L., Tao, S., Li, Y., and Lou, D.: Emission factors of particulate and
759 gaseous compounds from a large cargo vessel operated under real-world conditions,
760 *Environ. Pollut.*, 242, 667-674, <https://doi.org/10.1016/j.envpol.2018.07.036>, 2018a.
- 761 Huang, C., Hu, Q. Y., Li, Y. J., Tian, J. J., Ma, Y. G., Zhao, Y. L., Feng, J. L., An,
762 J. Y., Qiao, L. P., Wang, H. L., Jing, S. A., Huang, D. D., Lou, S. R., Zhou, M., Zhu, S.
763 H., Tao, S. K., and Li, L.: Intermediate Volatility Organic Compound Emissions from a
764 Large Cargo Vessel Operated under Real-World Conditions, *Environ. Sci. Technol.*, 52,
765 12934-12942, 10.1021/acs.est.8b04418, 2018b.
- 766 Hui, L., Liu, X., Tan, Q., Feng, M., An, J., Qu, Y., Zhang, Y., and Cheng, N.: VOC
767 characteristics, sources and contributions to SOA formation during haze events in
768 Wuhan, Central China, *Sci. Total. Environ.*, 650, 2624-2639,
769 10.1016/j.scitotenv.2018.10.029, 2019.
- 770 Ju, H.-j., and Jeon, S.-k.: Analysis of Characteristic Changes of Blended Very Low
771 Sulfur Fuel Oil on Ultrasonic Frequency for Marine Fuel, *J. Mar. Sci. Eng.*, 10, 1254,
772 2022.
- 773 Kawamura, K., Matsumoto, K., Uchida, M., and Shibata, Y.: Contributions of
774 modern and dead organic carbon to individual fatty acid homologues in spring aerosols
775 collected from northern Japan, *J. Geophys. Res-Atmos.*, 115, Artn D22310
776 10.1029/2010jd014515, 2010.
- 777 Kawamura, K., Hoque, M. M. M., Bates, T. S., and Quinn, P. K.: Molecular
778 distributions and isotopic compositions of organic aerosols over the western North
779 Atlantic: Dicarboxylic acids, related compounds, sugars, and secondary organic aerosol



- 780 tracers, *Org. Geochem.*, 113, 229-238,
781 <https://doi.org/10.1016/j.orggeochem.2017.08.007>, 2017.
- 782 Kleeman, M. J., Riddle, S. G., Robert, M. A., and Jakober, C. A.: Lubricating oil
783 and fuel contributions to particulate matter emissions from light-duty gasoline and
784 heavy-duty diesel vehicles, *Environ. Sci. Technol.*, 42, 235-242, [10.1021/es071054c](https://doi.org/10.1021/es071054c),
785 2008.
- 786 Knote, C., Hodzic, A., and Jimenez, J. L.: The effect of dry and wet deposition of
787 condensable vapors on secondary organic aerosols concentrations over the continental
788 US, *Atmos. Chem. Phys.*, 15, 1-18, [10.5194/acp-15-1-2015](https://doi.org/10.5194/acp-15-1-2015), 2015.
- 789 Kramel, D., Muri, H., Kim, Y., Lonka, R., Nielsen, J. B., Ringvold, A. L., Bouman,
790 E. A., Steen, S., and Strømman, A. H.: Global Shipping Emissions from a Well-to-Wake
791 Perspective: The MariTEAM Model, *Environ. Sci. Technol.*, 55, 15040-15050,
792 [10.1021/acs.est.1c03937](https://doi.org/10.1021/acs.est.1c03937), 2021.
- 793 Lehtoranta, K., Aakko-Saksa, P., Murtonen, T., Vesala, H., Ntziachristos, L.,
794 Ronkko, T., Karjalainen, P., Kuittinen, N., and Timonen, H.: Particulate Mass and
795 Nonvolatile Particle Number Emissions from Marine Engines Using Low-Sulfur Fuels,
796 Natural Gas, or Scrubbers, *Environ. Sci. Technol.*, 53, 3315-3322,
797 [10.1021/acs.est.8b05555](https://doi.org/10.1021/acs.est.8b05555), 2019.
- 798 Li, J., Zhang, Q., Wang, G., Li, J., Wu, C., Liu, L., Wang, J., Jiang, W., Li, L., Ho,
799 K. F., and Cao, J.: Optical properties and molecular compositions of water-soluble and
800 water-insoluble brown carbon (BrC) aerosols in northwest China, *Atmos. Chem. Phys.*,
801 20, 4889-4904, [10.5194/acp-20-4889-2020](https://doi.org/10.5194/acp-20-4889-2020), 2020.
- 802 Li, J. J., Wang, G. H., Ren, Y. Q., Wang, J. Y., Wu, C., Han, Y. N., Zhang, L., Cheng,
803 C. L., and Meng, J. J.: Identification of chemical compositions and sources of
804 atmospheric aerosols in Xi'an, inland China during two types of haze events, *Sci. Total*
805 *Environ.*, 566, 230-237, [10.1016/j.scitotenv.2016.05.057](https://doi.org/10.1016/j.scitotenv.2016.05.057), 2016.
- 806 Liang, Z., Yu, Z., Zhang, C., and Chen, L.: IVOC/SVOC and size distribution
807 characteristics of particulate matter emissions from a modern aero-engine combustor in
808 different operational modes, *Fuel.*, 314, [10.1016/j.fuel.2021.122781](https://doi.org/10.1016/j.fuel.2021.122781), 2022.
- 809 Liu, H., Meng, Z.-H., Lv, Z.-F., Wang, X.-T., Deng, F.-Y., Liu, Y., Zhang, Y.-N.,
810 Shi, M.-S., Zhang, Q., and He, K.-B.: Emissions and health impacts from global
811 shipping embodied in US-China bilateral trade, *Nat. Sustain.*, 2, 1027-1033,
812 [10.1038/s41893-019-0414-z](https://doi.org/10.1038/s41893-019-0414-z), 2019.
- 813 Liu, Z. Y., Chen, Y. J., Zhang, Y., Zhang, F., Feng, Y. L., Zheng, M., Li, Q., and
814 Chen, J. M.: Emission Characteristics and Formation Pathways of Intermediate Volatile
815 Organic Compounds from Ocean-Going Vessels: Comparison of Engine Conditions
816 and Fuel Types, *Environ. Sci. Technol.*, 56, 12917-12925, [10.1021/acs.est.2c03589](https://doi.org/10.1021/acs.est.2c03589),
817 2022.
- 818 Lou, H., Hao, Y., Zhang, W., Su, P., Zhang, F., Chen, Y., Feng, D., and Li, Y.:
819 Emission of intermediate volatility organic compounds from a ship main engine
820 burning heavy fuel oil, *J. Environ. Sci.*, 84, 197-204, [10.1016/j.jes.2019.04.029](https://doi.org/10.1016/j.jes.2019.04.029), 2019.
- 821 Mochida, M., Kitamori, Y., Kawamura, K., Nojiri, Y., and Suzuki, K.: Fatty acids
822 in the marine atmosphere: Factors governing their concentrations and evaluation of
823 organic films on sea-salt particles, *J. Geophys. Res-Atmos.*, 107, Artn 4325
824 [10.1029/2001jd001278](https://doi.org/10.1029/2001jd001278), 2002.
- 825 Mochida, M., Kawamura, K., Umemoto, N., Kobayashi, M., Matsunaga, S., Lim,
826 H. J., Turpin, B. J., Bates, T. S., and Simoneit, B. R. T.: Spatial distributions of
827 oxygenated organic compounds (dicarboxylic acids, fatty acids, and levoglucosan) in
828 marine aerosols over the western Pacific and off the coast of East Asia: Continental



- 829 outflow of organic aerosols during the ACE-Asia campaign, *J. Geophys. Res-Atmos.*,
830 108, Artn 8638
831 10.1029/2002jd003249, 2003.
- 832 Murphy, B. N., Woody, M. C., Jimenez, J. L., Carlton, A. M. G., Hayes, P. L., Liu,
833 S., Ng, N. L., Russell, L. M., Setyan, A., Xu, L., Young, J., Zaveri, R. A., Zhang, Q.,
834 and Pye, H. O. T.: Semivolatile POA and parameterized total combustion SOA in
835 CMAQv5.2: impacts on source strength and partitioning, *Atmos. Chem. Phys.*, 17,
836 11107-11133, 10.5194/acp-17-11107-2017, 2017.
- 837 Nadanakumar, V., Jenoris Muthiya, S., Prudhvi, T., Induja, S., Sathyamurthy, R.,
838 and Dharmaraj, V.: Experimental investigation to control HC, CO & NO_x emissions
839 from diesel engines using diesel oxidation catalyst, *Materials Today: Proceedings*, 43,
840 434-440, <https://doi.org/10.1016/j.matpr.2020.11.964>, 2021.
- 841 Organization, I. M.: International Convention for the Prevention of Pollution from
842 Ships, 2016.
- 843 Perrone, M. G., Carbone, C., Faedo, D., Ferrero, L., Maggioni, A., Sangiorgi, G.,
844 and Bolzacchini, E.: Exhaust emissions of polycyclic aromatic hydrocarbons, n-alkanes
845 and phenols from vehicles coming within different European classes, *Atmos. Environ.*,
846 82, 391-400, <https://doi.org/10.1016/j.atmosenv.2013.10.040>, 2014.
- 847 Reşitoğlu, İ. A., Altinişik, K., and Keskin, A.: The pollutant emissions from diesel-
848 engine vehicles and exhaust aftertreatment systems, *Clean Technol. Environ. Policy*, 17,
849 15-27, 10.1007/s10098-014-0793-9, 2015.
- 850 Robinson, A. L., Donahue, N. M., Shrivastava, M. K., Weitkamp, E. A., Sage, A.
851 M., Grieshop, A. P., Lane, T. E., Pierce, J. R., and Pandis, S. N.: Rethinking organic
852 aerosols: Semivolatile emissions and photochemical aging, *Science*, 315, 1259-1262,
853 10.1126/science.1133061, 2007.
- 854 Schüppel, M., and Gräbner, M.: Pyrolysis of heavy fuel oil (HFO) – A review on
855 physicochemical properties and pyrolytic decomposition characteristics for application
856 in novel, industrial-scale HFO pyrolysis technology, *J. Anal. Appl. Pyrolysis*, 179,
857 106432, 10.1016/j.jaap.2024.106432, 2024.
- 858 Shen, X. B., Che, H. Q., Yao, Z. L., Wu, B. B., Lv, T. T., Yu, W. H., Cao, X. Y.,
859 Hao, X. W., Li, X., Zhang, H. Y., and Yao, X. L.: Real-World Emission Characteristics
860 of Full-Volatility Organics Originating from Nonroad Agricultural Machinery during
861 Agricultural Activities, *Environ. Sci. Technol.*, 57, 10308-10318,
862 10.1021/acs.est.3c02619, 2023.
- 863 Shrivastava, P., and Nath Verma, T.: An experimental investigation into engine
864 characteristics fueled with Lal ambari biodiesel and its blends, *Therm. Sci. Eng. Prog.*,
865 17, 100356, <https://doi.org/10.1016/j.tsep.2019.100356>, 2020.
- 866 Sofiev, M., Winebrake, J. J., Johansson, L., Carr, E. W., Prank, M., Soares, J., Vira,
867 J., Kouznetsov, R., Jalkanen, J. P., and Corbett, J. J.: Cleaner fuels for ships provide
868 public health benefits with climate tradeoffs, *Nat. Commun.*, 9, 10.1038/s41467-017-
869 02774-9, 2018.
- 870 Srivastava, D., Vu, T. V., Tong, S. R., Shi, Z. B., and Harrison, R. M.: Formation
871 of secondary organic aerosols from anthropogenic precursors in laboratory studies, *npj*
872 *Clim. Atmos. Sci.*, 5, 10.1038/s41612-022-00238-6, 2022.
- 873 Su, P., Hao, Y., Qian, Z., Zhang, W., Chen, J., Zhang, F., Yin, F., Feng, D., Chen,
874 Y., and Li, Y.: Emissions of intermediate volatility organic compound from waste
875 cooking oil biodiesel and marine gas oil on a ship auxiliary engine, *J. Environ. Sci.*, 91,
876 262-270, 10.1016/j.jes.2020.01.008, 2020.



- 877 Wang, H., Hu, Q., Huang, C., Lu, K., He, H., and Peng, Z.: Quantification of
878 Gaseous and Particulate Emission Factors from a Cargo Ship on the Huangpu River, in:
879 *J. Mar. Sci. Eng.*, 8, 2023.
- 880 Wu, L., Wang, X., Lu, S., Shao, M., and Ling, Z.: Emission inventory of semi-
881 volatile and intermediate-volatility organic compounds and their effects on secondary
882 organic aerosol over the Pearl River Delta region, *Atmos. Chem. Phys.*, 19, 8141-8161,
883 10.5194/acp-19-8141-2019, 2019.
- 884 Wu, Z., Zhang, Y., He, J., Chen, H., Huang, X., Wang, Y., Yu, X., Yang, W., Zhang,
885 R., Zhu, M., Li, S., Fang, H., Zhang, Z., and Wang, X.: Dramatic increase in reactive
886 volatile organic compound (VOC) emissions from ships at berth after implementing the
887 fuel switch policy in the Pearl River Delta Emission Control Area, *Atmos. Chem. Phys.*,
888 20, 1887-1900, 10.5194/acp-20-1887-2020, 2020.
- 889 Xie, M., Wang, G., Hu, S., Han, Q., Xu, Y., and Gao, Z.: Aliphatic alkanes and
890 polycyclic aromatic hydrocarbons in atmospheric PM₁₀ aerosols from Baoji, China:
891 Implications for coal burning, *Atmos. Res.*, 93, 840-848,
892 <https://doi.org/10.1016/j.atmosres.2009.04.004>, 2009.
- 893 Yashnik, S. A., and Ismagilov, Z. R.: Diesel Oxidation Catalyst Pt–Pd/MnO_x–
894 Al₂O₃ for Soot Emission Control: Effect of NO and Water Vapor on Soot Oxidation,
895 *Topics in Catalysis*, 66, 860-874, 10.1007/s11244-022-01779-z, 2023.
- 896 Yu, G. Y., Zhang, Y., Yang, F., He, B. S., Zhang, C. G., Zou, Z., Yang, X., Li, N.,
897 and Chen, J.: Dynamic Ni/V Ratio in the Ship-Emitted Particles Driven by Multiphase
898 Fuel Oil Regulations in Coastal China, *Environ. Sci. Technol.*, 55, 15031-15039,
899 10.1021/acs.est.1c02612, 2021.
- 900 Zhang, F., Chen, Y. J., Tian, C. G., Wang, X. P., Huang, G. P., Fang, Y., and Zong,
901 Z.: Identification and quantification of shipping emissions in Bohai Rim, China, *Sci.*
902 *Total. Environ.*, 497, 570-577, 10.1016/j.scitotenv.2014.08.016, 2014.
- 903 Zhang, F., Chen, Y. J., Tian, C. G., Lou, D. M., Li, J., Zhang, G., and Matthias, V.:
904 Emission factors for gaseous and particulate pollutants from offshore diesel engine
905 vessels in China, *Atmos. Chem. Phys.*, 16, 6319-6334, 10.5194/acp-16-6319-2016,
906 2016.
- 907 Zhang, F., Chen, Y., Chen, Q., Feng, Y., shang, Y., Yang, X., Gao, H., Tian, C., Li,
908 J., Zhang, G., Matthias, V., and Xie, Z.: Real-World Emission Factors of Gaseous and
909 Particulate Pollutants from Marine Fishing Boats and Their Total Emissions in China,
910 *Environ. Sci. Technol.*, 52, 4910-4919, 10.1021/acs.est.7b04002, 2018a.
- 911 Zhang, F., Chen, Y. J., Su, P. H., Cui, M., Han, Y., Matthias, V., and Wang, G. H.:
912 Variations and characteristics of carbonaceous substances emitted from a heavy fuel oil
913 ship engine under different operating loads, *Environ. Pollut.*, 284, ARTN 117388
914 10.1016/j.envpol.2021.117388, 2021.
- 915 Zhang, F., Xiao, B., Liu, Z., Zhang, Y., Tian, C., Li, R., Wu, C., Lei, Y., Zhang, S.,
916 Wan, X., Chen, Y., Han, Y., Cui, M., Huang, C., Wang, H., Chen, Y., and Wang, G.:
917 Real-world emission characteristics of VOCs from typical cargo ships and their
918 potential contributions to secondary organic aerosol and O₃ under low-sulfur fuel
919 policies, *Atmos. Chem. Phys.*, 24, 8999-9017, 10.5194/acp-24-8999-2024, 2024.
- 920 Zhang, Y., Yang, W., Simpson, I., Huang, X., Yu, J., Huang, Z., Wang, Z., Zhang,
921 Z., Liu, D., Huang, Z., Wang, Y., Pei, C., Shao, M., Blake, D. R., Zheng, J., Huang, Z.,
922 and Wang, X.: Decadal changes in emissions of volatile organic compounds (VOCs)
923 from on-road vehicles with intensified automobile pollution control: Case study in a
924 busy urban tunnel in south China, *Environ. Pollut.*, 233, 806-819,
925 10.1016/j.envpol.2017.10.133, 2018b.



- 926 Zhao, W., Zhang, Y., Huang, G., He, Z., Qian, Y., and Lu, X.: Experimental study
927 of butanol/biodiesel dual-fuel combustion in intelligent charge compression ignition
928 (ICCI) mode: A systematic analysis at low load, *Fuel.*, 287, 119523,
929 <https://doi.org/10.1016/j.fuel.2020.119523>, 2021.
- 930 Zhao, Y., Hennigan, C. J., May, A. A., Tkacik, D. S., de Gouw, J. A., Gilman, J. B.,
931 Kuster, W. C., Borbon, A., and Robinson, A. L.: Intermediate-Volatility Organic
932 Compounds: A Large Source of Secondary Organic Aerosol, *Environ. Sci. Technol.*, 48,
933 13743-13750, 10.1021/es5035188, 2014.
- 934 Zhao, Y., Nguyen, N. T., Presto, A. A., Hennigan, C. J., May, A. A., and Robinson,
935 A. L.: Intermediate Volatility Organic Compound Emissions from On-Road Diesel
936 Vehicles: Chemical Composition, Emission Factors, and Estimated Secondary Organic
937 Aerosol Production, *Environ. Sci. Technol.*, 49, 11516-11526, 10.1021/acs.est.5b02841,
938 2015.
- 939 Zhao, Y., Nguyen, N. T., Presto, A. A., Hennigan, C. J., May, A. A., and Robinson,
940 A. L.: Intermediate Volatility Organic Compound Emissions from On-Road Gasoline
941 Vehicles and Small Off-Road Gasoline Engines, *Environ. Sci. Technol.*, 50, 4554-4563,
942 10.1021/acs.est.5b06247, 2016.
- 943 Zhou, S., Zhou, J., and Zhu, Y.: Chemical composition and size distribution of
944 particulate matters from marine diesel engines with different fuel oils, *Fuel.*, 235, 972-
945 983, 10.1016/j.fuel.2018.08.080, 2019.
- 946
947